The 2010 IEEE/RSJ International Conference on
Intelligent Robots and Systems
October 18-22, 2010, Taipei, Taiwan

Fractional Impedance Control for Reproducing the Material Properties of Muscle

Yo Kobayashi, *Member, IEEE*, Takeshi Ando, *Student Member, IEEE*,
Takao Watanabe, *Student Member, IEEE*, Masatoshi Seki and Masakatsu G. Fujie, *Member, IEEE*

***Abstract*— We reported a novel impedance control method based on a fractional calculation inspired by the viscoelastic properties of biomaterials such as muscle. This fractional impedance controller was found to realize superior impact absorption for the purpose of flexible contact for assistive and rehabilitation robots. This paper presents a preliminary evaluation of this concept using simulations and experiments. The numerical analysis results demonstrate that a fractional impedance controller has superior impact absorption performance than a conventional controller for contact with the elastic objects, especially for high stiffness objects and high velocity movement. The numerical analysis also reveals that using a fractional controller improved the robustness with respect to the robot dynamics. Moreover, the experimental results demonstrate that the fractional controller effectively suppresses the force between a person and a robot.**

I. Introduction

In recent years, research and development has been conducted on robots designed to assist people with disabilities in daily activities. However, these rehabilitation robots have not become popular yet. In contrast, industrial robots that specialize in accurately positioning solid targets with well-known mechanical properties are already prevalent. Unlike industrial robots, rehabilitation robots have to physically interact with people to assist them in their activities. If solid robots that only use position control are used it is possible to damage the robot and/or injure the person. Thus, rehabilitation robots require the ability to have a safe user-robot interaction by evaluating the response forces. There is a great demand for control technology for realizing flexible contact and cooperative behavior.

A. Related work

Force control is generally used to realize flexible contact and cooperative behavior in rehabilitation robots. Force control enables the virtual stiffness of the robot to be easily changed. This ability is crucial because the appropriate stiffness varies from person to person. One of the most popular approaches is impedance or admittance control [1], which generates a specific end-of-arm stiffness which has the form of impedance. For example, Krebs et al. proposed a rehabilitation robot that performs spatial extensions using impedance control [2]. Pledgie et al. developed an algorithm for suppressing tremors [3]. Blaya et al. present a variable impedance method for treating drop-foot gait [4]. Jezernik et al. developed algorithms for automatically adapting the motion of a robotic rehabilitation device [5]. Veneman et al. present an exoskeleton robot for interactive gait rehabilitation [6]. Watanabe et al. developed a force control method for a body-weight support system that provides support to the pelvis [7][8].

B. Problems

However, there are several technical challenges that need to be overcome for robots to realize flexible contact with people. A rehabilitation robot could behave unstably when in contact with a person. This problem arises from the fact that human movement support requires a large increase (or decrease) in the force in certain situations. It may cause a robot to impart a large impact force to a person in some situations. An unstable situation may also arise from the dynamic responses of robots. Rehabilitation robots are required to be as small as possible to ensure safety and good handleability. Thus, actuators are designed to be small and to consume little power. This may cause a robot to respond unstably, such as performing oscillations.

C. Objectives

Human arms and legs are better able to contact flexibly and absorb impact than robotic limbs. Many explanations have been proposed for why human limbs have this ability to absorb impact; these include the ability to adjust stiffness, feedforward control, and/or learning of the nervous system, and the presence of redundancies and polyarticular muscles.

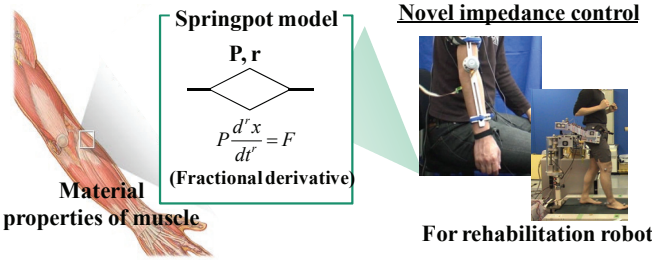

Fig.1: Concept of this study [8][9]

Manuscript received March 10, 2010. This work was supported in part by Global COE (Centers of Excellence) Program "Global Robot Academia," Waseda University, Tokyo, Japan and in part by Grant Scientific Research (A) (20240058), Japan

Y. Kobayashi is with Faculty of Science and Engineering, Waseda University, Japan. 59-309, 3-4-1, Ohkubo, Shinjuku, Tokyo (phone:+81-3-5286-3412; fax: +81-3-5291-8269; e-mail: you-k@fuji.waseda.jp).

M. Seki, T. Watanabe and T. Ando are with Graduate School of Science and Engineering, Waseda University, Japan.

M.G. Fujie is with Graduate School of Science and Engineering, Waseda University, Japan and Faculty of Science and Engineering, Waseda University, Japan.

However, the presence of redundancies and polyarticular muscles affect end-point stiffness properties of limbs but does not affect its dynamic characteristics. The large delay in the human neural system also restricts the effectiveness of stiffness adjustment and control systems for absorbing impact (Loop transmission delays are typically in the range 100–150 ms).

We consider that the viscoelasticity of muscle is one of the key factors for the ability of muscle to absorb impact and its robustness with respect to delay in control systems. We expect that these abilities stem from "special" dynamic properties of human muscle. In fact, researchers (including our group) have reported [10][11] that the viscoelasticity of a biomaterial has different properties from conventional serial and/or parallel arrangements of springs (stiffness) and dashpots (viscosity) considered in models such as Hill's model. These studies suggest that a "springpot", which is based on fractional calculus, accurately represents the viscoelastic properties of biomaterials, whereas the conventional viscoelastic model does not. (Fractional calculus is a branch of mathematical analysis concerned with taking real or complex number powers of differential operators.)

Based on the above discussion, we hypothesize that a controller that reproduces the viscoelastic properties of muscle will have a superior ability to realize flexible contact than a conventional controller. In this study, we propose using novel impedance control based on fractional calculus (the springpot model) to provide flexibleness of muscles for a robot. The controller is based on the impedance controller proposed by Hogan et al. [1], except the form of impedance. The form of impedance in our controller is represented by springpot model to reproduce the viscoelasticity of muscle. We call this method "fractional impedance control".

This present study investigates using a fractional controller to realize more flexible contact than that obtained using a conventional controller with spring–dashpot properties. This paper presents a preliminary evaluation of this concept based on simulations and experiments. We focus here on only the viscoelasticity of muscle and exclude other factors such as those mentioned above and the contractile element in Hill's model; these aspects will be considered in future studies.

The remainder of the paper is organized as follows. Section II describes measurement and modeling of the material properties of muscles. Section III presents formulation of simulation analysis. Section III examines the ability of our fractional controller by simulation while Section IV evaluates the controller by experiment. Finally, section V summarizes the conclusions of this study and describes future work.

II. Measurement and Modeling of Viscoelastic Properties of Muscle

We have studied biomechanical modeling of the viscoelastic properties of liver [11]. We modeled the viscoelastic properties using a single fractional derivative term. This model accurately reproduced the viscoelastic properties at low frequencies. We developed a viscoelastic muscle model based on this modeling method. In this section, we report measurement and modeling of the viscoelastic properties of muscles of hogs and evaluate whether the model is suitable for muscle tissue. We have previously reported the material properties of a hog liver [11] and gave detailed descriptions of this modeling method. Thus, this paper gives only a brief description of the material behavior.

A. Method

The following experiments were individually conducted to measure the physical properties of a hog interior muscle tissue (tender loin) using a rheometer (TA Instruments: AR-G2). The shear modulus, shear stress, and shear strain were then calculated based on these measurements. A dynamic viscoelastic test was performed to measure the frequency response of the muscle tissue. Sinusoidal stress with angular frequencies in the range 0.1 to 10 rad/s (giving a strain amplitude of 3%) was applied to the tissue. From the results of this test, we obtained the mechanical impedance (the storage elastic modulus G_s, and the loss elastic modulus G_l) .

B. Result and Modeling

Figure 2 shows the experimental results of the dynamic viscoelastic tests. In a previous study using a hog liver [11], we showed that viscoelastic properties of the liver can be modeled using the fractional derivative expressed in (1), which considers only the low-frequency characteristics:

$$G\frac{d^r\gamma}{dt^r}=\tau \tag{1}$$

where G is the viscoelasticity, t is the time, γ is the shear strain, r is the order of the derivative, and τ is the shear stress. The parameters in (1) were adjusted to fit the experimental results shown in Fig. 2. Figure 2 also shows the viscoelastic properties of the model that were obtained using (1). For reference, Fig. 2 also shows the viscoelastic properties of conventional spring–dashpot model as modeled using (2):

$$\alpha\gamma+\eta\frac{d\gamma}{dt}=\tau \tag{2}$$

where α is the elasticity and η is the viscosity. Table I shows the values of all the parameters in (1) and (2).

C. Discussion

These results reveal that the viscoelastic properties of the hog muscle tissue and those of the fractional model have similar tendencies. Therefore, the model based on (1) can accurately reproduce the viscoelastic responses of muscle tissue. The fractional order r is equal to 0.15 based on the slopes of G_c and G_l in Fig. 2 (This value for the fractional order (0.15) was used for the fractional impedance controller in next section.) In contrast, the conventional spring-dashpot model cannot fit the viscoelastic properties of muscle (Fig. 2(b)).

The fractional and conventional modeling results differ mainly in the loss elastic modulus G_l. Compared with G_l for the fractional model, the G_l for the conventional spring–dashpot model increases rapidly as the frequency increases. It is clear from (2) that the slope of the loss modulus predicted by the spring–dashpot model will be 1.0 in a

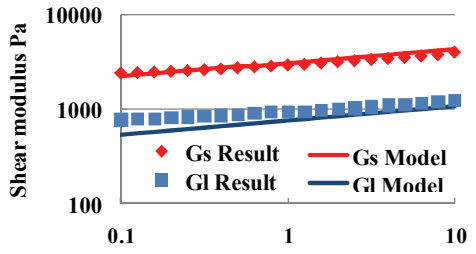

(a) Experimental result and fractional model

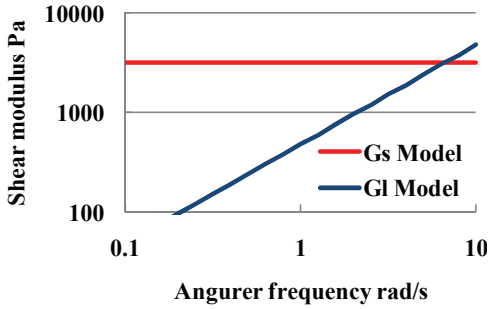

(b) spring-dashpot (Voight) model

Fig. 2: Experimental result of mechanical impedance. G_c is the storage elastic modulus, and G_l is the loss elastic modulus. The red and blue plots are the experimental result and the red and blue lines are the responses of the model.

Table I Value of each parameter in (1) and (2)

	G	*r*	K	*C*
Fractional model	3200	0.15		
spring-dashpot model			3200	480 (=3200 x 0.15)

log–log plot. In contrast, the measured slope for a muscle was 0.15. Thus, spring–dashpot models are practically useless for modeling the viscoelastic properties when the loss elastic modulus G_l exhibits a weak frequency dependence, such as for the experimental results in this study. We expect that this difference in the frequency dependences will affect the ability.

III. FORMULATION AND GOVERNING EQUATION

We propose a fractional impedance controller, which has a fractional form of the impedance represented in (1). The objective of this study is to compare the impact absorption abilities of the fractional controller and a conventional controller, which has the spring–dashpot properties represented in (2). Conventional impedance controllers generally include a mass term. For simplicity, we omit the mass term in this analysis to facilitate comparison with the fractional controller (1), which does not have a mass term.

Figures 3 and 4 present the analysis model and its block diagram, respectively. The analysis model consists of the "dynamic response of the robot", the "impedance controller" and the "contact object". For simplicity, we assume the following linear, time-invariant, one-dimensional system. The robot is controlled by position-based impedance control. The contact object collides with the robot. The impedance

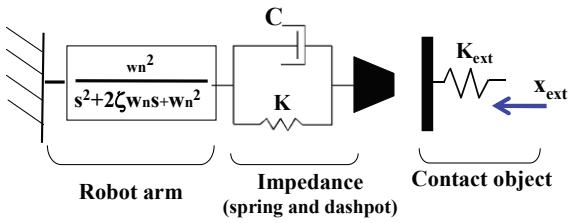

(a) Conventional impedance control with spring and dashpot

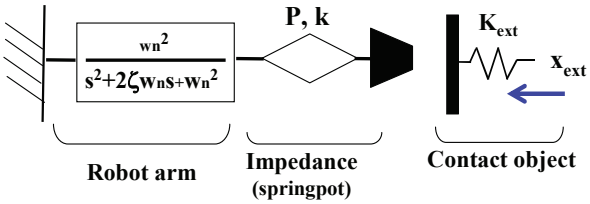

(b) Fractional impedance control with springpot

Fig. 3 Conceptual scheme of the analysis model

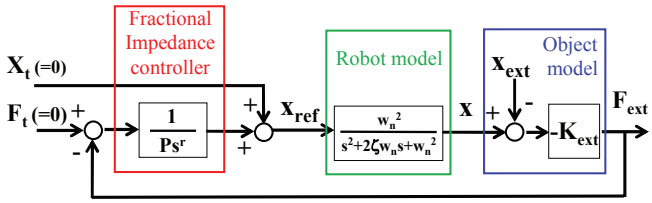

(a) Conventional impedance control with spring and dashpot

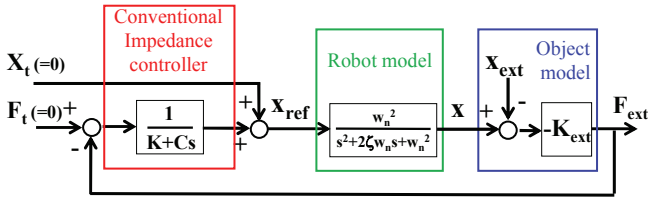

(b) Fractional impedance control with springpot

Fig.4 Block diagram of the analysis model

controller generates motion to reduce the contact force between the end effector and the object. The robot dynamics give rise to a certain delay in the reference position of the controller. We evaluate the force between the object and the robot.

A. Analysis model

1) Robot dynamics: The dynamics of a robot is typically modeled using a second-order nonlinear model. However, the dynamics of a robot actuated by a DC or AC motor with high-resolution gears can be linearized because the interference of each joint becomes negligible. For simplicity, we assume that inertial and viscous damping of the joints dominates the robot dynamics. The differential equation are then given by:

$$\frac{d^2x}{dt^2} + 2\zeta w_n \frac{dx}{dt} + w_n{}^2 x = w_n{}^2 x_{ref} \qquad (3)$$

where x is position of end effector, w_n is natural frequency, ζ is damping ratio, t is time, x_r is reference position of end effector.

2) Impedance controller: We implemented position-based impedance control (admittance control), which is actually a position controller nested within a force feedback loop. Force feedback is employed in the target impedance model to modify the reference position. We used two impedance controllers in the evaluation. One impedance controller is a conventional controller that consists of a spring and a dashpot connected in parallel. The differential equation for this impedance controller is given by:

$$Kx_{ref} + C\frac{dx_{ref}}{dt} = f_{ext}(t) \tag{4}$$

where C is the virtual viscosity, K is the virtual stiffness, R (=C/K) is the ratio of the viscosity to the stiffness, x_{ref} is the reference position of the end effector, x is the actual position of the end effector and f_{ext} is the force between the contact object and the end effector.

The other impedance controller is designated to reproduce the viscoelastic properties of muscle using a springpot model, as expressed by (1). The differential equation of this impedance controller is respectively given by:

$$P\frac{d^r x_{ref}}{dt^r} = f_{ext}(t) \tag{5}$$

where P represent visoelasticity, r represent fractional parameter of springpot.

3) Contact object: the elastic contact object collide to the end-effector of robot. We assume the position of contact object is given as following equation:

$$x_{ext}(t) = x_s(1 - \exp(-t/\tau)) \tag{6}$$

where x_{ext} is the (external) position of the contact object, x_s is its steady-state position, and τ is the time constant of the system. This modeling is based on the motion of human limbs when a person moves an arm or leg from one position to another. An example of this motion is given in section V.

B. Equation

The force generated between the end effector and the contact object is described by:

$$f_{ext}(t) = -K_{ext}(x - x_{ext}) \tag{7}$$

where f_{ext} is the external force, K_{ext} is the stiffness of the contact object, x is the position of the end effector, and x_{ext} is the position of the contact object.

1) Spring–dashpot impedance controller: From (4) and (7), the differential equation between x_{ext} and x_{ref} is given by:

$$(1 + \frac{K}{K_{ext}})x_{ref} + \frac{K}{K_{ext}}\frac{C}{K}\frac{dx_{ref}}{dt} = x_{ext}(t) \tag{8}$$

Normalized equation of (8) is give as

$$(1 + A)x_{ref} + AR\frac{dx_{ref}}{dt} = x_{ext}(t) \tag{9}$$

$$A = \frac{K}{K_{ext}} \quad R = \frac{C}{K} \tag{10}$$

where A is the ratio of the stiffness of the impedance controller to that of the contact object and R is the ratio of the viscosity to the stiffness.

2) Fractional impedance control: From (5) and (7), the differential equation between x_{ext} and x_{ref} is given by:

$$K_{ext}x_r + P\frac{d^r x_r}{dt^r} = K_{ext}x_{ext}(t) \tag{11}$$

Normalized equations of (11) are given by:

$$x_{ref} + a\frac{d^r x_{ref}}{dt^r} = x_{ext}(t) \tag{12}$$

$$a = \frac{P}{K_{ext}} \tag{13}$$

where a is the ratio of the stiffness of the impedance controller to that of the contact object and r is the fractional parameter of springpot (i.e., the viscosity ratio in the springpot model).

IV. Model Analysis

A. Methods

We analyzed the system performances of the conventional and fractional impedance controllers. We performed time-domain analysis in this evaluation. We compared the force response of each controller for the following states of the contact object and the robot:

1) Viscosity ratio in impedance controller (R and r): We compared the fractional and conventional controllers using the same values for R in (9) and r in (12) because both parameters have a similar definition (i.e., viscosity ratio) in each controller. Based on the viscoelastic properties of muscle tissue described in section II, R and r for the impedance controllers were set to 0.15. We report here the analysis for when the fractional parameter of springpot r is 0.15, which is based on the muscle properties. Obviously, fractional impedance control with using a different value for the fractional parameter r (including variable impedance control) is conceivable and may generate new insights. This will be investigated in future studies.

2) Stiffness ratio (A and a): We analyzed the force response with three different stiffness ratios A and a. Specifically, the stiffness ratios A and a were set to 0.1, 1.0, and 10.0.

3) System time constant of contact object motion τ: We also analyzed the force response with four different system time constants τ (1, 10, 20, and 100).

4) Dynamic response of robot: We analyzed the force response with three different natural frequencies w_n (10, 30, and 100). We also conducted the analysis when the robot's position is close to the reference position, the output from the impedance controller (i.e., $w_n = \infty$, $G(s) = 1$, and $x = x_{ref}$). On the other hand, we set the damping ratio ζ for the robot dynamics to be 1.0, for simplicity.

As shown in 1)–4), the parameters that determine the force response are {w_n, A (or a), τ} in this investigation. We repeatedly calculated the external force for each impedance controller by changing these parameters.

B. Results and Discussion

1) Stiffness ratio A and a: Figure 5 displays the results for the external force f_{ext} when the natural frequency $w_n = \infty$ rad/s, the system time constant τ = 20 ms, and the stiffness ratios have the following values: A and a=0.1 (Fig. 5(a)), A and a=1.0 (Fig. 5(b)), and A and a=10 (Fig. 5(c)). Figure 5 shows

that for each value of A and a the maximum external force f_{ext} was lower when the fractional impedance controller was used. The fractional controller results also reveal that the overshoot remained low for all values of the stiffness ratio. The force with conventional impedance control becomes large as the stiffness ratio increases. These results reveal that the fractional controller provides better impact absorption than the conventional controller. Specifically, the results in this paragraph show that the fractional controller has superior impact absorption for an elastic object that has a high stiffness.

2) System time constant of contact object motion τ: Figure 6 shows the results for the external force f_{ext} when the natural frequency of the contact object motion $w_n = \infty$ rad/s, the stiffness ratio A and $a = 1.0$ and the system time constant has the following values: τ=100 ms (Fig. 6(a)), 10 ms (Fig. 6(b)), 1 ms (Fig. 6(c)). For each value of τ, the maximum external force f_{ext} was lower when the fractional controller was used. The impedance controllers made little difference to the external force f_{ext} when the input (external position x_{ext}) is slow (e.g., τ = 100 ms). However, the response made a difference when the input became rapid (e.g., τ = 10 and 1 ms). In particular, fractional controller did not overshoot when τ = 10 ms, whereas the response of the conventional controller had a large overshoot. The results in this paragraph demonstrate that for rapid input (external position x_{ext}) the response f_{ext} of the fractional controller is superior to that of the conventional controller.

3) Dynamic response of robot: Figure 7 shows the results for the external force f_{ext} when the stiffness ratio A and $a = 1.0$, the system time constant τ = 20 ms, and the natural frequency has the following values: w_n = 100 rad/s (Fig. 7(a)), 30 rad/s (Fig. 7(b)), and 10 rad/s (Fig. 7(c)). For each value of w_n, the

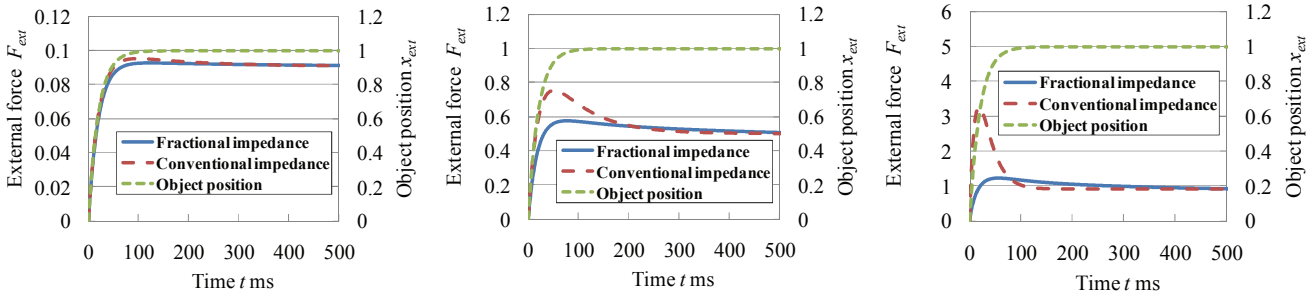

(a) $\{w_n,\ A(\text{ or } a),\ \tau\} = \{\infty, 0.1, 20\}$ (b) $\{w_n,\ A(\text{ or } a),\ \tau\} = \{\infty, 1.0, 20\}$ (c) $\{w_n,\ A(\text{ or } a),\ \tau\} = \{\infty, 10, 20\}$

Fig. 5 Result of time-domain analysis for various stiffness ratio a and A.

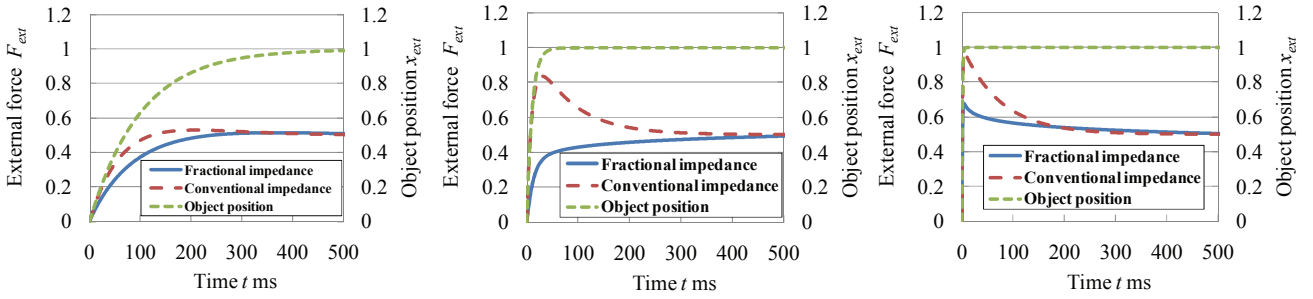

(a) $\{w_n,\ A(\text{ or } a),\ \tau\} = \{\infty, 1.0, 100\}$ (b) $\{w_n,\ A(\text{ or } a),\ \tau\} = \{\infty, 1.0, 10\}$ (c) $\{w_n,\ A(\text{ or } a),\ \tau\} = \{\infty, 1.0, 1\}$

Fig. 6 Result of time-domain analysis for various system time constant of contact object motion τ

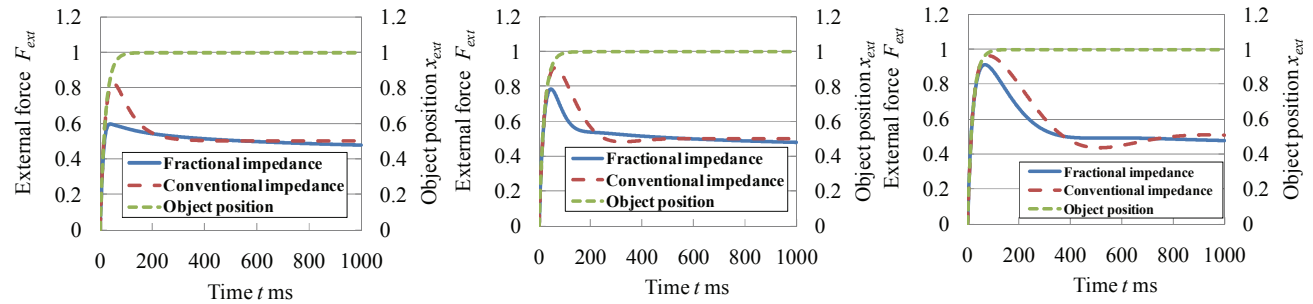

(a) $\{w_n,\ A(\text{ or } a),\ \tau\} = \{100, 1.0, 20\}$ (b) $\{w_n,\ A(\text{ or } a),\ \tau\} = \{30, 1.0, 20\}$ (c) $\{w_n,\ A(\text{ or } a),\ \tau\} = \{10, 1.0, 20\}$

Fig.7 Result of time-domain analysis for various robot dynamics response w_n.

maximum external force f_{ext} was lower when fractional controller was used. The external force f_{ext} of the fractional controller at w_n = 100 rad/s is approximately the same as that at $w_n = \infty$ rad/s shown in Fig. 5(b), whereas there is a significant difference between the response at w_n = 100 rad/s and $w_n = \infty$ rad/s for the conventional controller. The fractional impedance controller overshoots the force f_{ext}, but it does not undershoot it. The force f_{ext} of the conventional controller generated oscillations (i.e., both overshoots and undershoots). These results suggest that the fractional controller is more robust with respect to the dynamic response of robot than the conventional controller.

V. EXPERIMENT

A. Objectives

This section describes the preliminary experiment to evaluate fractional impedance control. We implemented fractional and conventional controllers in actual robots and measured their impact absorption performances. We performed the following experiment to evaluate a fractional impedance controller, supposing that the controller was implemented in a joint of an arm exoskeleton robot for ensuring flexible contact and cooperative behavior with people.

B. Method

Figure 8 depicts the conceptual scheme and experimental setup. The manipulator had one degree of freedom. A position-controlled actuator was attached to rotate the handle. A six-axis force/torque sensor was attached to the base of the handle. The angle of the handle θ(= the angle of actuator) was impedance-controlled corresponding to the force perpendicular to the axis of the arm. Both fractional and conventional impedance controllers were individually implemented in this manipulator. The stiffness ratios A and a of these impedance controllers were set to 0.15, as in the numerical analysis. The magnitudes of the controllers K and P were set to approximately 30 N/rad, based on trial and error.

A healthy young subject was told to twist the handle at two subjectively determined angular velocities: low (about 0.1 rad/s) and high (about 0.5 rad/s). Thus, the external angle θ_{ext} was input to the robot from the subject. The manipulator was placed on a table and the subject stood next to the table. The subject twisted the handle by moving his forearm, while keeping his upper arm almost stationary. The separate experiments were performed for the conventional and fractional controllers. The force imparted to the handle and the angle θ were measured in each experiment.

Table II compares the parameters used in the model analysis in section IV and those of the experiment in this section.

C. Result and Discussion

Figure 9 shows the experimental results for the low angular velocity. The experimental results for the angle θ reveal that the subject rotated the handle in the same manner in the both experiments. The results show that the force f_x for the conventional controller increased sharply and overshoot. In contrast, the force f_x for the fractional controller does not increase sharply or overshoot and was lower than that for the conventional controller.

Figure 10 shows the experimental result for the high angular velocity. The results for the angle θ show that the subject rotated the handle in the same manner in both experiments. The results show that the force f_x for the conventional controller increased sharply and overshoot. In contrast, the force f_x for the fractional controller does not increase sharply or overshoot and was lower than that for the conventional controller.

Table II Correspondence table

	Model analysis	Experiment
Position of end effector (handle)	x	θ
Reference position of end effector (handle)	x_{ext}	θ_{ref}
Position of contact object (hand)	x_{ext}	θ_{ext}
Force between contact object and end effector	f_{ext}	f_x

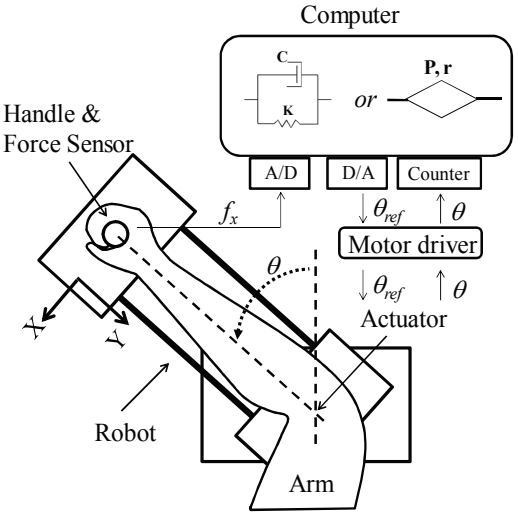

(a) conceptual scheme

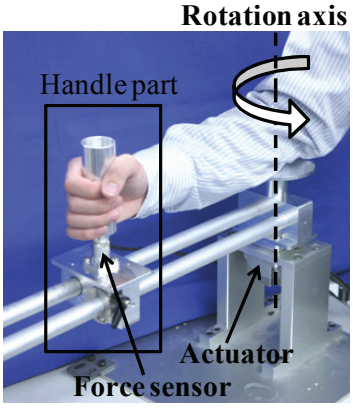

(b) experimental setup

Fig.8 conceptual schema and setup of the experiment

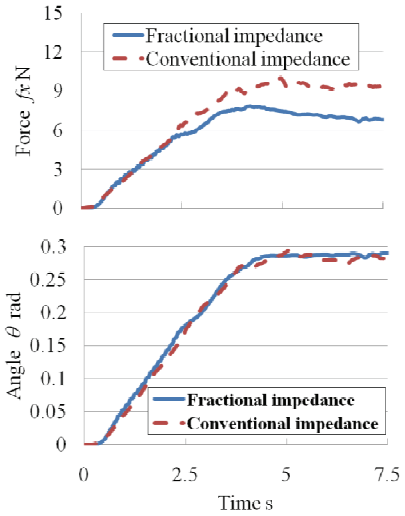

Fig.9 Experimental result with low angular velocity

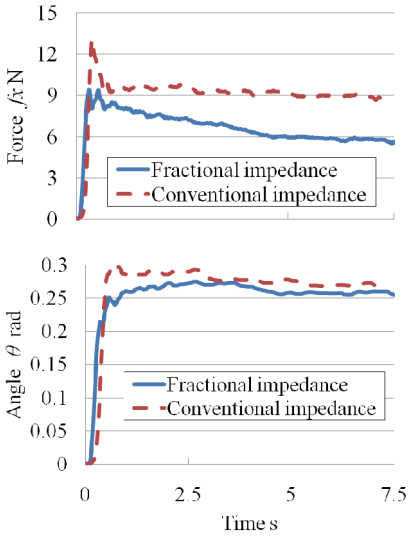

Fig.10 Experimental result with high angular velocity

These results suggest that the conventional controller has inferior flexible contact with a person than the fractional controller because the controller generates large impacts for high-velocity input. In contrast, the fractional controller did not generate a large force during the experiments. This result suggests that a fractional controller has superior performance for flexible contact with human arm movement.

VI. Conclusions and Future Work

We reported a novel impedance control method based on a fractional calculation inspired by the viscoelastic properties of biomaterials such as muscle. This fractional impedance controller was found to realize superior impact absorption for the purpose of flexible contact for assistive and rehabilitation robots. This paper presents a preliminary evaluation of this concept using simulations and experiments. The numerical analysis results demonstrate that a fractional impedance controller has superior impact absorption performance than a conventional controller for contact with the elastic objects, especially for high stiffness objects and high velocity movement. The numerical analysis also reveals that using a fractional controller improved the robustness with respect to the robot dynamics. Moreover, the experimental results demonstrate that the fractional controller effectively suppresses the force between a person and a robot.

However, evaluation of its steady-state performance and robustness with respect to sensor noise remains a task for further investigation. We reported here the analysis for when the fractional parameter of the springpot r is 0.15. The fractional impedance control with different values of the fractional parameter r (including variable impedance control) is conceivable and may generate new insights. Moreover, fractional impedance control with serial and/or parallel arrangements of springpot models has the potential to realize better and efficient performance. We intend to address these challenges in future studies. We also intend to implement and evaluate a fractional controller in a rehabilitation or assistive robot.

References

[1] N. Hogan, “Impedance control: An approach to manipulation: Part i, ii and iii,” Journal of Dynamic Systems, Measurement and Control, vol. 107, no. 1, pp. 1–23, 1985.

[2] H. I. Krebs, M. Ferraro, S Buerger1, M. J. Newbery, A. Makiyama, M. Sandmann, “Rehabilitation robotics: pilot trial of a spatial extension for MIT-Manus”, Journal of NeuroEngineering and Rehabilitation 2004, 1:5 doi:10.1186/1743-0003-1-5

[3] T. Pledgie, K. E. Barner, S. K. Agrawal, T. Rahman, “Tremor suspression through impedance control”, IEEE transactions on rehabilitation engineering, Vol.8, no.1, 2000

[4] J. A. Blaya and H. Herr, “Adaptive Control of a Variable-Impedance Ankle-Foot Orthosis to Assist Drop-Foot Gait”, IEEE transactions on Neural Systems and Rehabilitaion Engineering, Vol. 12, No. 1, pp. 24-31, 2004

[5] S. Jezernik, G. Colombo and M. Morari, “Automatic Gait-Pattern Adaptation Algorithms for Rehabilitation With a 4-DOF Robotic Orthosis”, IEEE Transaction on Robotics and Atomation, Vol. 20, No. 3, pp.574-582, 2004

[6] J. F. Veneman, R. Kruidhof, E. E. G. Hekman, R. Ekkelenkamp, E. H. F. Van Asseldonk and H. van der Kooij, “Design and Evaluation of the LOPES Exoskeleton Robot for Interactive Gait Rehabilitation”, I IEEE transactions on Neural Systems and Rehabilitaion Engineering, Vol.15, No.3, pp.378-386, 2007

[7] T. Watanabe, E. Ohki, T. Ando, M. G. Fujie, “Fundamental study of force control method for pelvis-supporting body weight support system,” Proceedings of the 2008 IEEE International Conference on Robotics and Biomimetics, 2008

[8] T. Watanabe, E. Ohki, Y. Kobayashi, M. G. Fujie, “Leg-dependent Force Control for Body Weight Support by Gait Cycle Estimation from Pelvic Movement,” Proceedings of the 2010 IEEE International Conference on Robotics and Automation, accepted, 2010

[9] T. Ando, M. Watanabe and M. G. Fujie, ” Extraction of voluntary movement for an EMG controlled exoskeltal robot of tremor patients”, 4th International IEEE/EMBS Conference on Neural Engineering, pp.120-123, 2009

[10] R.L. Magin, Fractional calculus models of complex dynamics in biological tissues, Computers and Mathematics with Applications (2009), doi:10.1016/j.camwa.2009.08.039

[11] Y. Kobayashi, J. Okamoto, M. G. Fujie, “Physical Properties of the Liver and the Development of an Intelligent Manipulator for Needle Insertion” , in Proceedings of 2005 IEEE International Conference on Robotics and Automation, pp.1644-1651, 2005